New Journal of Physics
The open-access journal for physics

High-viscosity fluid threads in weakly diffusive microfluidic systems

T Cubaud[1,3] **and T G Mason**[2]

[1] Department of Mechanical Engineering,
Stony Brook University, Stony Brook, NY 11794, USA
[2] Department of Chemistry and Biochemistry, Department of Physics and Astronomy, and California NanoSystems Institute, University of California—Los Angeles, Los Angeles, CA 90095, USA
E-mail: thomas.cubaud@stonybrook.edu

New Journal of Physics **11** (2009) 075029 (14pp)
Received 23 February 2009
Published 31 July 2009
Online at http://www.njp.org/
doi:10.1088/1367-2630/11/7/075029

Abstract. We provide an overview of the flow dynamics of highly viscous miscible liquids in microfluidic geometries. We focus on the lubricated transport of high-viscosity fluids interacting with less viscous fluids, and we review methods for producing and manipulating single and multiple core-annular flows, i.e. viscous threads, in compact and plane microgeometries. In diverging slit microchannels, a thread's buckling instabilities can be employed for generating ordered and disordered miscible microstructures, as well as for partially blending low- and high-viscosity materials. The shear-induced destabilization of a thread that flows off-center in a square microchannel is examined as a means for continuously producing miscible dispersions. We show original compound threads and viscous dendrites that are generated using three fluids, each of which has a large viscosity contrast with the others. Thread motions in zones of microchannel extensions are examined in both miscible and immiscible environments. We demonstrate that high-viscosity fluid threads in weakly diffusive microfluidic systems correspond to the viscous primary flow and can be used as a starting point for studying and understanding the destabilizing effects of interfacial tension as well as diffusion. Characteristic of lubricated transport, threads facilitate the transport of very viscous materials in small fluidic passages, while mitigating dissipation. Threads are also potentially promising for soft material synthesis and diagnostics with independent control of the thread specific surface and residence time in micro-flow reactors.

[3] Author to whom any correspondence should be addressed.

Contents

1. Introduction

In recent years, microfluidic research has focused in part on the realization of micro-reactions between fluids compromised of various molecules and particulates, the size of which can be comparable to the dimension of the reacting chamber [1]–[3]. Streams can have complex time-dependent compositions and concentrations, and overall exhibit widely different viscosities. However, transport, synthesis and diagnostics of high-viscosity and soft materials in small fluidic passages remain challenging due to the high resistance to flow and the need to develop methods for manipulating streams having large viscosity contrasts in microfluidic devices.

The creation of a viscous-core annular flow provides a compelling solution for reducing the energy cost required to pump and manipulate thick materials with solvents in hydraulic systems [4]. The tendency for low viscosity constituents to stratify into the regions of high shear and form a lubrication layer, which can envelop high-viscosity constituents, has numerous implications in science and engineering, such as in volcanic conduits [5], lubricated pipelining [6] and multi-component polymeric flows [7]–[9]. Miscible core-annular flows are also sometimes compared to their immiscible counterparts [10], and numerous studies of flows and displacements using miscible fluids have shown a variety of microstructures, including 'corkscrew', 'pearl and mushroom', 'finger', 'spike' and 'tendril' in Hele-Shaw cells, tubes and microgravity experiments [11]–[17]. Variation in the different specific devices and gravitational effects, however, make it difficult to compare the results obtained, and this difficulty has thus inhibited the creation of a unifying picture of the free-boundary flow dynamics.

Here, we experimentally investigate miscible multi-fluid flows using fluids having large viscosity contrasts in elementary microfluidic designs. In particular, we focus on the spatial arrangement and stability of lubricated threads having a high viscosity coefficient in fast, yet laminar, convective flows. For short intervals of time, high-viscosity fluids can behave as solids [18] and slender viscous structures, such as threads [19]–[25] and sheets [26]–[29], can buckle in a fashion similar to elastic solids. Using continuous flows, we review how buckling instabilities can be exploited in microfluidic devices to produce ordered and disordered miscible microstructures. We investigate the formation of viscous threads in compact and plane geometries and study folding and coiling instabilities in diverging microchannels. The shear-induced breakup of a continuous thread into discrete elements is examined in square microchannels. We also describe novel spatial arrangements of three-fluid flows and

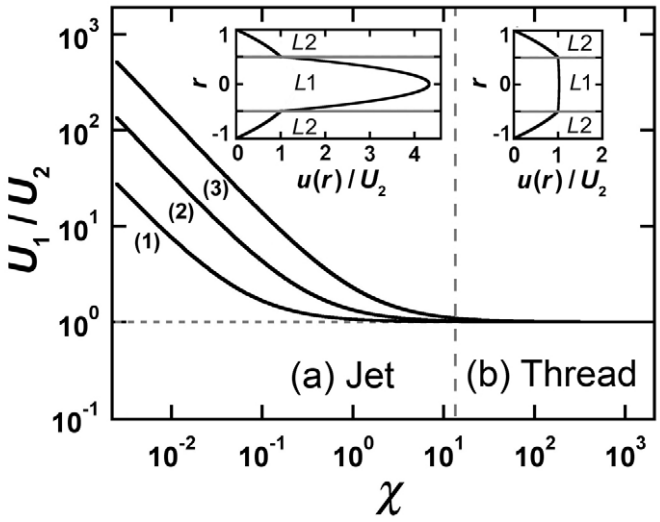

Figure 1. Evolution of the core maximal velocity U_1 normalized by the annulus maximal velocity U_2 versus viscosity contrast χ for dimensionless core radius $c = (1)\ 0.25$, (2) 0.50 and (3) 0.75. In region (a), the parabolic velocity profile in the core is typical of a jet (inset: velocity profile for $\chi = 10^{-1}$ and $c = 0.5$). In region (b), the uniform velocity profile in the core is typical of a thread (inset: velocity profile for $\chi = 15$, $c = 0.5$).

demonstrate the formation of compound threads and viscous dendrites. Finally, we compare the morphology of miscible and immiscible high-viscosity threads in microchannel extensions.

2. Core-annular flows

'Threads' are typically referred to as extruded fluid streams that have a core moving in solid-like motion, and 'jets' as fluid streams that move faster than the surrounding fluid into which they are injected. For the case of a core-annular flow in a circular tube of radius R, jets and threads can be distinguished based on the viscosity ratio between the core (liquid $L1$) and the annulus (liquid $L2$): $\chi = \eta_1/\eta_2$. The velocity profile for the basic flow can be directly calculated from the Stokes equations [6, 13] and expressed in dimensionless form according to:

$$u = \begin{cases} u_1 = \frac{1}{\chi}(c^2 - r^2) + 1 - c^2, & \text{for } 0 \leqslant r \leqslant c, \\ u_2 = 1 - r^2, & \text{for } c \leqslant r \leqslant 1, \end{cases} \tag{1}$$

where the radial coordinate r and the core radius c are normalized by R, and $u_i = V_i(4\eta_2)/[(\nabla P)R^2]$ is the dimensionless velocity in region i, ∇P is the pressure gradient, and V_i is the velocity in region i. Figure 1 shows the evolution of the maximum velocity ratio U_1/U_2, with $U_1 = u_1(r = 0)$ and $U_2 = u_2(r = c)$, between the core and the annulus versus χ for three core radii $c = 0.25$, 0.5 and 0.75. The regime for large χ corresponds to a thread having a uniform velocity profile, i.e. $U_1 \approx U_2$, and the regime for small χ corresponds to a jet having a parabolic velocity profile, i.e. $U_1 > U_2$. Although the transition is smooth, the data suggest a cut-off value around $\chi \approx 15$. The velocity gradient at the interface of the thread and annulus

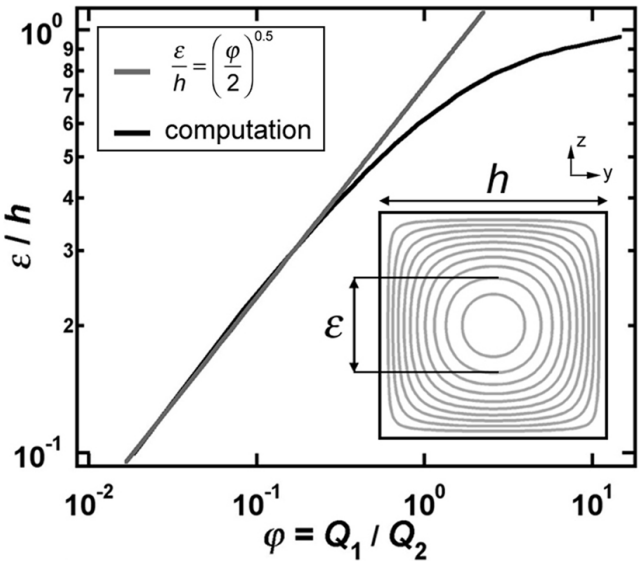

Figure 2. Evolution of core diameter ε/h versus flow rate ratio φ for a thread in plug flow in a square microchannel. Inset: cross-sectional contour plot of a set of iso-velocity contours in a square duct calculated using Fourier analysis.

is smoother than for the case of a jet, which strongly affects the stability of the core in both miscible [6, 30] and immiscible [31, 32] environments.

The relationship between c and the flow rate ratio $\varphi = Q_1/Q_2$ of each liquid is calculated by integrating equation (1) across the area of each region, yielding:

$$\varphi = \frac{c^4(\chi^{-1} - 2) + 2c^2}{(1 - c^2)^2}. \tag{2}$$

In the regime associated with small threads $c \ll 1$ and large viscosity ratios $\chi \gg 1$, a simple scaling for the thread can be made: $c \sim (\varphi/2)^{1/2}$. Although this analysis is only valid for a circular tube, it gives a simple estimate for the behavior of core annular flows as a function of the viscosity contrast. For the case of a square microchannel of width h, the relationship between the thread diameter ε and φ can be computed numerically using the contour plot of the velocity field in a square duct [33] assuming a core in plug flow (figure 2). Using $\varepsilon/h = c$ for comparing circular and square cross sections, data show that the relationship between ε/h and φ is essentially the same for both tubes when $\chi \gg 1$ and scales as $\varepsilon/h \sim (\varphi/2)^{1/2}$ for small threads.

The main result from this analysis in the asymptotic regime reveals that a core can be transported within a less viscous annulus, independent of absolute viscosities, provided $\chi > 15$. This simple property offers significant advantages for manipulating high-viscosity materials at small scales. The behavior of weakly diffusive threads in simple microgeometries is of both practical and fundamental interest because it corresponds to the basic viscous primary flow and provides a basis for comparing the modifying effects of molecular diffusion or interfacial tension. Weakly diffusive regimes are readily accessible experimentally; high-viscosity liquid pairs generally have a small molecular diffusion coefficients D, so Péclet numbers $Pe = U_1 h/D$ are large, i.e. $Pe > 10^3$. In the following, we present an overview of our investigations on high-viscosity threads in weakly diffusive microfluidic systems.

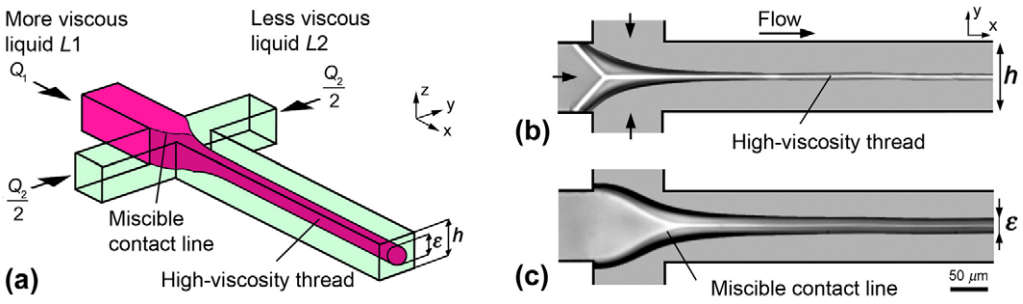

Figure 3. Formation of miscible high-viscosity fluid threads. (a) Schematics of compact hydrodynamic focusing section. Experimental micrographs of miscible high-viscosity thread formation for $\chi = 83$, (a) $\varphi = 0.01$ and (b) $\varphi = 0.20$.

3. Thread formation

To experimentally study high-viscosity threads, we fabricate hard microfluidic modules using glass and silicon. Microchannel designs are lithographically patterned onto a double-sided polished silicon wafer ($h = 100\,\mu$m) that is etched-through using deep reactive ion etching. Each side of the silicon slab is then anodically bonded to a piece of glass, providing a glass/silicon/glass sandwich structure that can sustain high-pressure and is chemically resistant. Since the microchannel's sidewalls are made of silicon and the top and bottom walls are made of glass, these devices are transparent normal to the flow direction. To visualize flows, a fiber light is placed on one side of the module and a high-speed camera equipped with a high magnification lens is located on the opposite side. We use syringe-pumps to infuse conventional polydimethylsiloxane (PDMS) oils (i.e. silicone oils), having a wide range of viscosities between 0.5 and 4865 cP, into the devices. These silicone oils are fully miscible since they differ only in molecular weight.

Threads can be readily produced using a symmetric hydrodynamic focusing section, which consists of four microchannels with square-cross sections of identical width h that intersect at right angles (figure 3(a)). The more viscous liquid 1 ($L1$), having viscosity η_1, is introduced into the inlet channel at the volumetric flow rate Q_1, and the less viscous liquid ($L2$), having a viscosity η_2, is introduced at the inlet of the two side channels with a total flow rate Q_2. In the weakly diffusive regime, when $\chi = \eta_1/\eta_2 \geqslant 15$ and $\varphi = Q_1/Q_2 < 0.8$, $L2$ wraps around $L1$ in the outlet channel and $L1$ forms a high-viscosity thread that fully detaches from the edge of the walls (figures 3(b) and (c)). The optical signature of the thread encapsulation by $L2$ is given by the presence of steady-state miscible contact lines on the glass substrate. As φ increases, the morphology of miscible contact lines evolves toward a curved 'V' pointing toward the flow direction. We found previously that the thread diameter ε/h was independent of χ and followed $\varepsilon/h \sim \varphi^{0.6}$ [34]. Using the same geometry, we have also measured the thread diameter of capillary threads [31] and found good agreement with the expected behavior $\varepsilon/h \sim (\varphi/2)^{1/2}$. Since, over the range of diameters experimentally measured, the discrepancy between these laws only arises for large threads $\varepsilon/h > 0.5$, we suspect that diffusive effects, which can smear out the boundary regions, may have played a small role in the measurements for large threads. Overall, compact hydrodynamic focusing into a square microchannel provides an efficient way to produce high-viscosity threads in both miscible and immiscible environments.

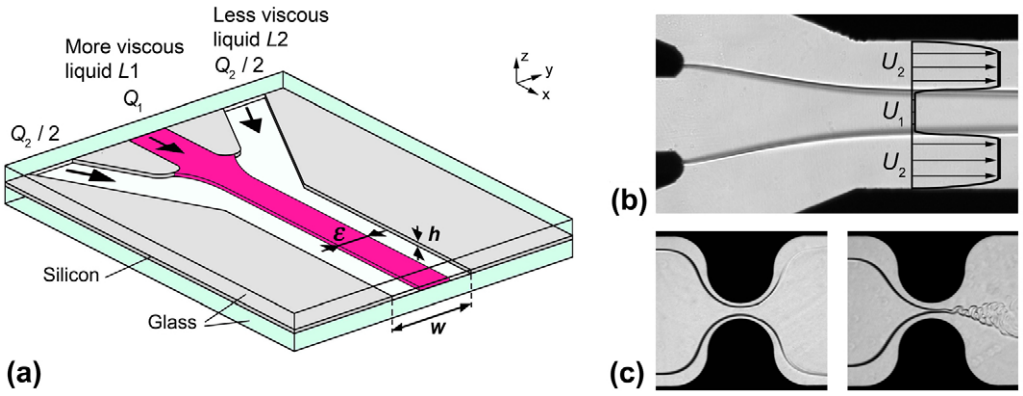

Figure 4. Hydrodynamic focusing in a plane geometry. (a) Schematic of a viscous layered flow in a plane geometry. (b) Experimental micrograph of stratified bulk velocity profiles that have not detached from upper and lower glass walls: $\chi = 610$ and $\varphi = 3.3 \times 10^{-3}$. (c) Thread formation (i.e. detachment of the more viscous fluid from all walls) and buckling in a constriction, $\chi = 610$, $\varphi = 0.03$ (left) and $\varphi = 0.01$ (right).

Lubricated transport of high-viscosity fluids is characteristic of compact channels, such as circular or square ducts. In plane geometries, however, highly viscous fluids are more likely to contact top and bottom walls, with significant dissipation resulting. Using a similar injection scheme, we have investigated hydrodynamic focusing into a plane microchannel [35] having a large aspect ratio $w/h = 20$, where w and h were the width and height of the channel, respectively (figure 4(a)). Using the Hele-Shaw approximation, the relationship between the bulk velocities of $L1$ and $L2$ can be estimated as $U_1 = U_2/\chi$, so the more viscous central stream has a much lower velocity than the less viscous side flows (figure 4(b)). Experimentally, the width of the central strip ε is in good agreement with $\varepsilon/w = [1 + (\chi\varphi)^{-1}]^{-1}$ for large widths $\varepsilon > 2h$. For thin widths, $\varepsilon < 2h$, viscous encapsulation effects become significant and the previous expression overestimates ε. We also investigate the influence of a constriction of width $w_c = 2h$ on the path of a viscous layered flow and observe that a thread could be formed in the constriction below a critical flow rate ratio φ_c (figure 4(c)). Interestingly, in the diverging channel region, downstream from the constriction, the newly formed thread experiences a viscous buckling instability [35].

4. Folding and coiling

Diverging slit microchannels form a group of simple microfluidic designs that provide a transition zone between compact and planar (i.e. quasi-two-dimensional) geometries. These channels are ideal for producing multi-fluid buckling instabilities. Slender viscous structures, when considered over short intervals of time, can exhibit dynamic responses to stress reminiscent of elastic solids. For the flows that we study, a characteristic convective time scale t is set by the flow of $L2$ such that $t \sim 1/\gamma_2$, where γ_2 is the shear rate of $L2$. Applying shear stress continuity at the thread boundary simply yields $\gamma_1 = \gamma_2/\chi$, where γ_1 is the shear rate of $L1$. Hence, the thread-flow time scale $t_1 \sim 1/\gamma_1 \sim \chi t$ is much larger than the convective

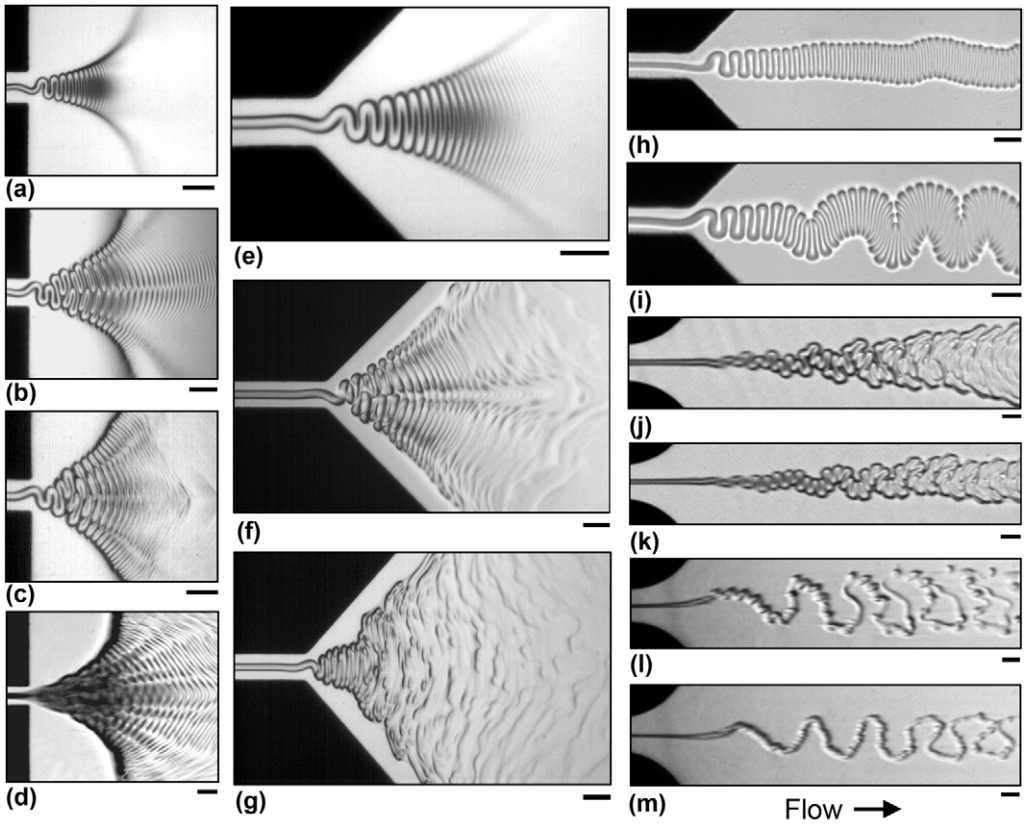

Figure 5. Buckling of weakly diffusive threads in diverging channels between silicone oils (scale bars: 100 μm). (a) Folding, $\varphi = 0.2$, $\chi = 83$. Subfolding: (b) $\varphi = 0.24$, $\chi = 400$. (c) $\varphi = 0.2$, $\chi = 400$. (d) $\varphi = 0.22$, $\chi = 400$. (e) Folding $\varphi = 0.29$, $\chi = 83$. (f) Subcoiling: $\varphi = 0.2$, $\chi = 1000$. (g) Coiling: $\varphi = 0.1$, $\chi = 1000$. Secondary folding: (h) $\varphi = 0.15$, $\chi = 520$, (i) $\varphi = 0.22$, $\chi = 520$, (j) $\varphi = 0.038$, $\chi = 122$, (k) $\varphi = 0.033$, $\chi = 122$, (l) $\varphi = 0.016$, $\chi = 122$ and (m) $\varphi = 0.011$, $\chi = 122$.

time scale. In other words, the thread transported in the fast flow field of $L2$ 'does not have enough time to flow', and, as a result, can effectively behave as an amorphous solid. In the control volume of the diverging channel, the thread primarily bends and coils while conserving mass rather than simply dilating by enlarging its core diameter. This buckling due to deceleration of the core is similar to the buckling that occurs when viscida decelerate as they impinge into a solid surface.

Microfluidic viscous buckling morphologies are remarkably diverse and depend on many parameters, including the thread diameter ε, diverging channel angle α, viscosity contrast χ, initial thread confinement, thread velocity U_1, and diffusion coefficient D. Figure 5 displays typical microstructures for weakly diffusive threads. Large threads are mainly restricted to fold in two-dimensions, whereas smaller threads can experience both folding and coiling in three-dimensions. In long diverging channels, the deformed structure of $L1$ eventually makes contact with the top and bottom glass walls and forms a pile downstream. In this situation, the peak amplitude defines a nearly parabolic envelope that becomes wider as α and/or ε increase. The folding oscillation frequency f measured at the end of the square channel is directly proportional

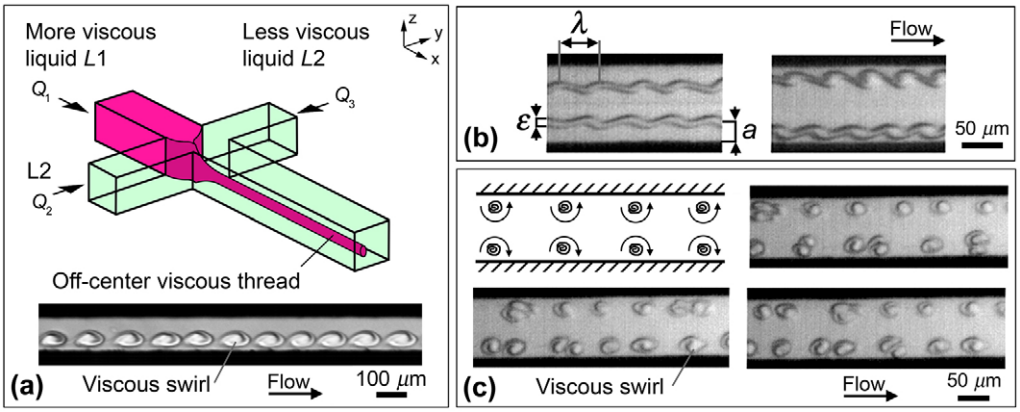

Figure 6. Viscous swirling instability. (a) Schematic of single off-center thread formation and micrograph of an array of swirls for $\chi = 83$ and flow rates in μl min^{-1}: $Q_1 = 1$, $Q_2 = 2$, $Q_3 = 10$. (b) Development of perturbations having a characteristic wavelength λ along two off-center threads of diameter ε at a distance a from the sidewalls. Micrographs for $\chi = 83$: $\lambda/\varepsilon \approx 4.2$, $a/h \approx 0.26$ (left), $\lambda/\varepsilon \approx 2.8$, $a/h \approx 0.16$ (right). (c) Schematic and micrographs of swirls tumbling in a square microchannel for $\chi = 83$.

to the characteristic shear rate of $L2$, $\gamma_2 \sim U_2/(h/2)$, and we find $f \sim \gamma_2/4$, which shows a strong dependence on Q_2 and a weak dependence on Q_1 [34].

The diversity and complexity of these patterns arise in part as a result of the dynamics of the fast lubricated thread impinging on and feeding the slowly convected pile; the thread's velocity is $U_1 \approx U_2$ while the pile's velocity is typically on the order of U_2/χ, according to studies of layered flows in the plane geometries [35]. Complex transient morphologies, such as subfolding, on the period-doubling path to chaotic deposition into the pile are also observed [34]. Subfolding is characterized by periodic alternation of folds in branches (figures 5(b)–(d)) and we show here that this phenomenon can also occur when the thread is coiling (figure 5(f)). The coiling configuration produces a pile morphology that is strongly heterogeneous in viscosity since $L2$ is directly injected through the coiling tube into the pile. Another structure of interest, which we label secondary folding (figures 5(i)–(m)), corresponds to a low frequency oscillation f_s of the pile or lubricated thread, such as when $f_s/f < 10^{-1}$. Overall, the large increase of interfacial area during folding and coiling instability makes it a model system for further investigating partial mixing between low- and high-viscosity components.

5. Viscous swirls

The possibility of breaking up high-viscosity threads into discrete elements in continuous flow regimes offers an innovative means for structuring and mixing microflows. Exploiting microfluidic laminar flow properties, the position of a thread inside a square microchannel can be adjusted. Single and multiple threads, which flow off-center in a square microchannel, can be generated using a different injection scheme [36]. For instance, here, we show that a small single thread can be made off-center from the channel by asymmetrical side-channel injection of $L2$ with $Q_3 > Q_2 > Q_1$ (figure 6(a)). Off-center threads are found to assume

an ellipsoidal cross-sectional area. Downstream, we observe sinuous perturbations having a characteristic wavelength λ in the direction transverse to the flow (figure 6(b)). We interpret these perturbations as the result of the competition between the viscous torque, due to the difference in drag on each side of a thread in the quasi-parabolic flow of $L2$, and its dynamic viscous bending resistance. Balancing the moments at the onset of the instability, we have developed a simple relationship for the slenderness ratio of the undulations, $\lambda/\varepsilon \approx C\chi/(1 - 2a/h)$, where $C = 4.7 \times 10^{-2}$ is a geometrical constant and a is the closest distance to the sidewalls. For the case of two co-flowing threads [36], this functional relationship yielded good agreement with experimental data for $C_{\text{exp}} \approx 2.8 \times 10^{-2}$ and $\chi = 83$. Eventually, undulations amplify and threads breakup into linear arrangements of discrete viscous swirls, miscible equivalents of droplets. Nascent swirls grow on the sinuous thread by collecting the high-viscosity liquid into central bulbs and depleting the regions in between them, which thin and are reminiscent of tails. Tails, eventually, become so thin they blend into the surrounding fluid, thereby separating neighboring swirls. After detaching from one another, swirls gain angular momentum and rotate, as expected for objects in a shear field (figure 6(c)). This intriguing shear-induced breakup of high-viscosity threads demonstrates the possibility of generating discrete diffusive elements at the microscale using continuous flows.

6. Compound threads and dendrites

Motivated by the concept of multiple-viscosity flow-segregation processes, we explore several novel flow configurations using several symmetrical cross-flow injection schemes. Liquids are now indexed symmetrically from the center of the channel outward depending on their respective injection points, i.e. $L1$ is the core fluid, $L2$ is the intermediate fluid, and the last liquid is at the sidewalls. Using two different oils, we have demonstrated the possibility of forming and coupling two nearby threads in a diverging channel [36]. The same behavior is observed with three threads in a spider-shaped junction (figure 7(a)).

We investigate multi-fluid flow with three different oils, which we label V (viscous), M (medium), and F (fluid), having the viscosity contrasts: $\eta_V/\eta_M > 15$ and $\eta_M/\eta_F > 15$. By permuting the injection points of these fluids using a tri-symmetrical injection scheme, we obtain six basic configurations. In order to form structures lubricated from the walls, however, one needs to require that $\eta_2/\eta_3 > 15$, which restricts us to three configurations of liquids ($L1$, $L2$, $L3$) that we label *VMF*, *MVF* and *FVM*. The configuration *VMF* leads to the formation of compound threads that can fold into a folding envelope (figures 7(b) and (c)). The morphology depends strongly on the flow rates. The configuration *MVF* produces a thread with a 'soft core', i.e. a core that can flow faster than the edge of the compound jet but slower than the external fluid. As a result, the core partially tempers buckling instabilities (figures 7(d) and (e)).

The last configuration, *FVM*, is of particular interest since it produces viscous dendrites. Since the less viscous oil is at the center (i.e. $L1 = F$) two asymmetrical threads of V form on each side of F and are surrounded by M. As a result, each thread folds asymmetrically in F and M, yielding intricate and meandering flows reminiscent of fin-shaped dendrite structures that grow as the flow proceeds downstream (figure 8). Here, the structure has a 'fluid core' that can flow faster than both the edges (V) and the surrounding fluid (M), so it strongly reduces or inhibits buckling instabilities in the center of the structure. The growth of viscous dendrites in a direction transverse to the main flow is an example of miscible displacement related to the classic Saffman–Taylor fingering instability. The layered structures that we observe suggest

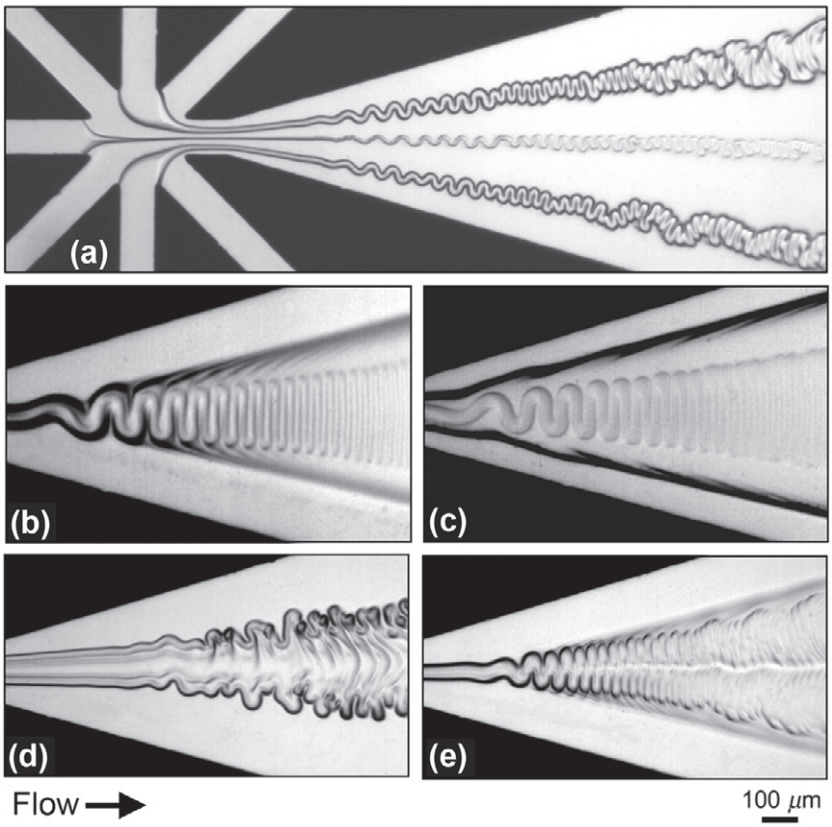

Figure 7. Micrographs of multiple and compound threads. Fluids: silicon oils, viscosities in cP, flow rates in μl min^{-1}. (a) Three threads: $(\eta_1, \eta_2, \eta_3, \eta_4) = (500, 6, 500, 6)$, $(Q_1, Q_2, Q_3, Q_4) = (1, 20, 5, 20)$. (b) Configuration *VMF*: $(\eta_1, \eta_2, \eta_3) = (500, 20, 0.5)$, $(Q_1, Q_2, Q_3) = (1, 5, 50)$. (c) Configuration *VMF*: $(\eta_1, \eta_2, \eta_3) = (500, 20, 0.5)$, $(Q_1, Q_2, Q_3) = (5, 15, 80)$. (d) Configuration *MVF*: $(\eta_1, \eta_2, \eta_3) = (20, 500, 0.5)$, $(Q_1, Q_2, Q_3) = (10, 5, 100)$. (e) Configuration *MVMF*: $(\eta_1, \eta_2, \eta_3, \eta_4) = (20, 500, 20, 0.5)$, $(Q_1, Q_2, Q_3, Q_4) = (5, 5, 5, 100)$.

similarities with large-scale geophysical processes that can involve molten rock, such as the folding of viscous layers [37] and lava flows [38].

Viscous encapsulation processes are promising for producing complex shell structures and multiple core-annular flows from basic hydrodynamic focusing geometries. This method for producing complex miscible flow patterns is comparable to the formation of multiple-emulsions using coaxial assemblies of capillary tubes [39], which in that particular case facilitate the formation of immiscible core-annular flows at small viscosity contrasts. Our study, which emphasizes large viscosity contrasts, suggests that complex dispersions can be formed using multiple immiscible core-annular flows in simple microfluidic networks.

7. Microfluidic extensional flows

Integrated microfluidics require the use of innovative device geometries, in which flow phenomena can be produced in precise and compact locations. Extensional flows produced by

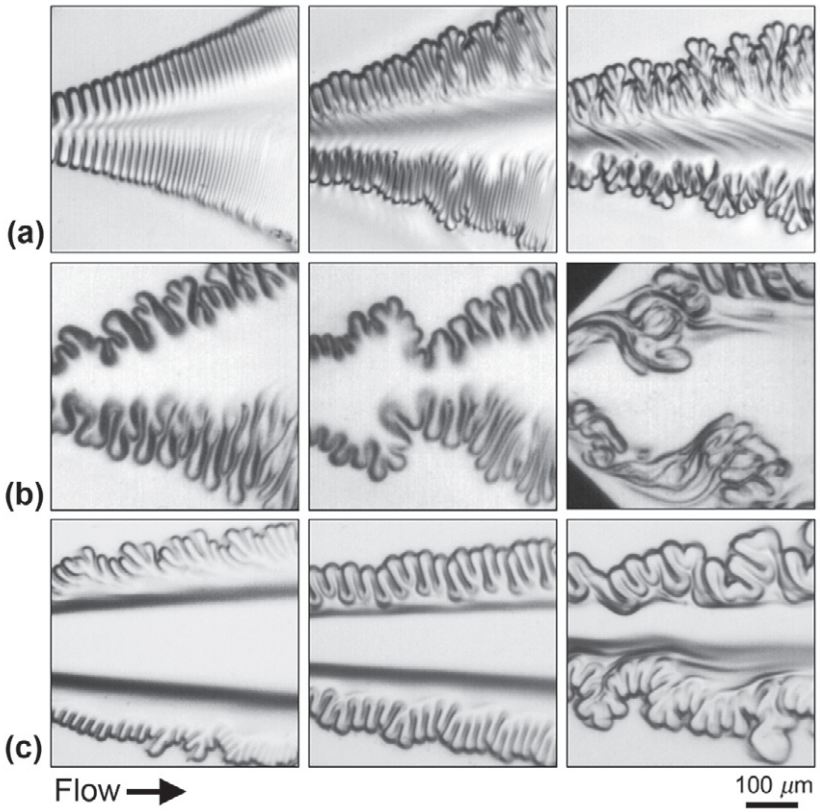

Figure 8. Micrographs of viscous dendrites, configuration *FVM*. Fluids: silicon oils; viscosities in cP; flow rates in μl min^{-1}; (from left to right). (a) $\eta_1 = 0.5$, $\eta_2 = 500$, $\eta_3 = 6$; $(Q_1, Q_2, Q_3) = (0.5, 5, 20)$, $(10, 15, 55)$, $(10, 15, 100)$. (b) $\eta_1 = 0.5$, $\eta_2 = 500$, $\eta_3 = 6$; $(Q_1, Q_2, Q_3) = (10, 0.5, 20)$, $(10, 0.5, 20)$, $(20, 10, 25)$. (c) $\eta_1 = 0.82$, $\eta_2 = 500$, $\eta_3 = 6$; $(Q_1, Q_2, Q_3) = (50, 2, 10)$, $(25, 3, 10)$, $(30, 9, 30)$.

diverging and converging microchannel geometries are advantageous because they can facilitate the direct comparison between fluid physicochemical properties and flow morphologies in a single field of view. We investigate thread motion in diamond-shaped diverging-converging slit microchannels connected by straight square microchannels (figure 9(a)). Using both miscible and immiscible fluids, we provided a direct visual comparison between the effects of diffusion or interfacial tension on the buckled structure of threads as they traverse the extension [40]. Here, figures 9(b) and (c) display related structures of threads made of high-viscosity silicone oil ($\eta_1 = 4865$ cP) in a miscible environment for a large Péclet number and in an immiscible environment for a large capillary number. These morphologies are characteristically seen when a thin film of $L2$ exists between the threads and the walls. Indeed, given the small thread diameters and the relatively small distance d between the extension's inlet and outlet, threads do not pile up against the top and bottom walls. For the immiscible case, the regular array of folds appears more rounded and fewer folds form due to the significant role of interfacial tension, which tends to reduce the interfacial area. In this pattern formation study, we have used primarily aquatic animal names to label the rich variety of flow morphologies in the diamond diverging-converging channel, yielding an 'aquarium' [40].

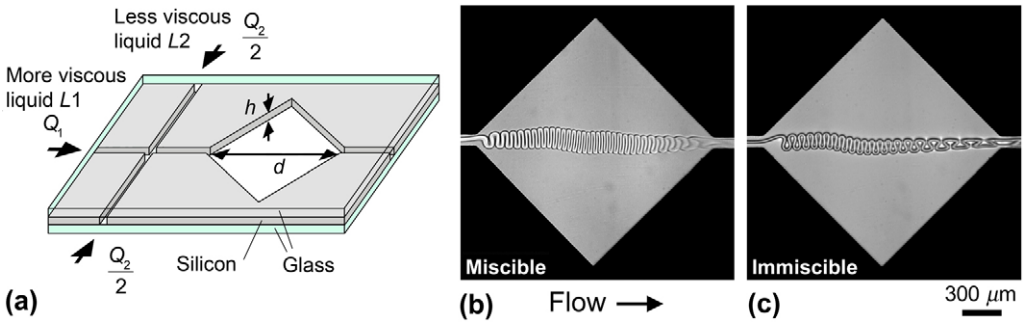

Figure 9. Thread motion in microchannel diverging-converging 'mirror symmetric' extensional flow geometries. (a) Schematic of a 'microfluidic aquarium', $h = 100\,\mu$m and $d = 2$ mm. (b) Folding of a lubricated thread in a miscible environment (i.e. negligible interfacial tension). Fluids: silicone oils, $\chi = 520$, $\varphi = 0.31$. (c) Folding of a lubricated thread in an immiscible environment (i.e. non-negligible interfacial tension). Fluids: silicone oil and isopropanol, $\chi = 2143$, $\varphi = 0.13$.

This diverging-converging extensional flow geometry offers the possibility to precisely investigate the condition for pile formation using rates of injection as control parameters. At the onset of lubrication failure, the thin film of $L2$ between the thread and the wall can either partially mix with $L1$ or be squeezed out from the pile in the miscible case. In contrast, for immiscible fluids, the film can rupture by nucleation of dewetting patches. This 'mirror geometry' design for a microfluidic cell could also potentially be useful for investigating the reversibility of low Reynolds number flows [41] with fluid–fluid interfaces and its implication for the nearly symmetrical thread deformations in the diverging and in the converging sections. Our exploration of these effects in conjunction with viscous buckling merely hints at the vast range of microstructured flows that can be formed using this simple geometry.

8. Conclusion

In this paper, we have reviewed and presented a wide variety of original flow effects that surround the formation and stability of high-viscosity fluid threads in the weakly diffusive regime using basic microfluidic geometries. Characteristic of lubricated transport, threads facilitate the transport of very viscous material in small fluidic passages while mitigating dissipation. Threads are also promising for soft material synthesis and diagnostics, since the relationship between diameter and flow rate ratio permits, in principle, the independent control of the thread's specific surface and residence time in micro-flow reactors. In addition, the thread's configuration in the weakly diffusive regime is equivalent to the two-fluid primary flow problem, and this can serve as a reference point for further studying the impact of destabilizing effects of diffusion between miscible fluids or interfacial tension between immiscible fluids. We have demonstrated a wide range of buckling phenomena that can be used for partially blending low- and high-viscosity constituents as well as for generating novel miscible dispersions. Injecting three fluids having large differences in viscosities into two cross-channels in series, we have revealed a host of intriguing multi-fluid arrangements. A powerful advantage of microfluidic manipulation of miscible flows is the possibility to explore flows without a

typifying length-scale. This situation is clearly different from immiscible flows, where surface tension prohibits any scaling above the capillary length, typically a few millimeters. By contrast, with miscible flows, applying known scaling approaches can potentially extend the relevance of our observations up to the macroscopic scale, and these flows suggest that geological processes could potentially be investigated using microfluidics of steadily injected viscous materials without unwanted complications introduced by gravitational acceleration and volumes of materials at larger scales. On a much smaller scale, flows of threads in microchannel extensional slit geometries offer a preview of interesting possibilities for manipulating thin films and producing forced wetting phenomena in new configurations. In addition to scaling analysis, more thorough theoretical and numerical analyses, including convection-diffusion treatments, would provide significant insights into the emergence of these complex viscous patterns yet produced by laminar flows with steady state upstream conditions. Finally, this study offers a promising means for further controlling rheological and structural properties of multi-component materials at small scales and for manipulating highly viscous biological and industrial fluids in future applications.

References

[1] Stone H A, Stroock A D and Ajdari A 2004 *Annu. Rev. Fluid Mech.* **36** 381
[2] Squires T M and Quake S R 2005 *Rev. Mod. Phys.* **77** 977
[3] deMello A J 2006 *Nature* **442** 394
[4] Joseph D D, Nguyen K and Beavers G S 1984 *J. Fluid Mech.* **141** 319
[5] Carrigan C R and Eichelberger J C 1990 *Nature* **343**
[6] Joseph D D and Renardy Y Y 1993 *Fundamentals of Two-Fluid Dynamics. Part II: Lubricated Transport, Drops and Miscible Liquids* (New York: Springer)
[7] Everage A E 1973 *Trans. Soc. Rheol.* **17** 629
[8] Khomami B and Su K C 2000 *J. Non-Newton. Fluid Mech.* **91** 59
[9] Karami A and Balke S T 2000 *Polym. Eng. Sci.* **40** 2342
[10] Selvam B, Merk S, Govindarajan R and Meiburg E 2007 *J. Fluid. Mech.* **592** 23
[11] Homsy G M 1987 *Annu. Rev. Fluid Mech.* **19** 271
[12] Lajeunesse E, Martin J, Rakotomalala N, Salin D and Yortsos Y C 1999 *J. Fluid Mech.* **398** 299
[13] Cao Q, Ventresca A L, Sreenivas K R and Prasad A K 2003 *Can. J. Chem. Eng.* **81** 913
[14] Rashidnia N, Balasubramaniam R and Schroer R T 2004 *Ann. New York Acad. Sci.* **1027** 311
[15] d'Ocle M, Martin J, Rakotomalala N, Salin D and Talon L 2008 *Phys. Fluids* **20** 024104
[16] Balasubramaniam R, Rashidnia N, Maxworthy T and Kuang J 2005 *Phys. Fluids* **17** 052103
[17] Schmidt L E and Zhang W W 2008 *Phys. Rev. Lett.* **100** 044502
[18] Landau L D and Lifshitz E M 1986 *Theory of Elasticity* (Oxford: Pergamon)
[19] Buckmaster J D 1973 *J. Fluid Mech.* **61** 449
[20] Cruickshank J O and Munson B R 1981 *J. Fluid Mech.* **113** 221
[21] Griffiths R W and Turner J S 1988 *Geophys. J.* **95** 397
[22] Mahadevan L, Ryu W S and Samuel A D T 1998 *Nature* **392** 140
[23] Maleki M, Habibi M, Golestanian R, Ribe N M and Bonn D 2004 *Phys. Rev. Lett.* **93** 214502
[24] Chiu-Webster S and Lister J R 2006 *J. Fluid Mech.* **569** 89
[25] Pouligny B and Chassande-Mottin M 2008 *Phys. Rev. Lett.* **100** 154501
[26] Suleiman S M and Munson B R 1981 *Phys. Fluids* **24** 1
[27] Skorobogatiy M and Mahadevan L 2000 *Europhys. Lett.* **52** 532
[28] Ribe N M 2002 *J. Fluid Mech.* **457** 255
[29] Ribe N M 2003 *Phys. Rev.* E **68** 036305

[30] d'Olce M, Martin J, Rakotomalala N, Salin D and Talon L 2009 *J. Fluid Mech.* **618** 305
[31] Cubaud T and Mason T G 2008 *Phys. Fluids* **20** 053302
[32] Guillot P, Colin A and Ajdari A 2008 *Phys. Rev.* E **78** 016307
[33] White F M 1991 *Viscous Fluid Flow* (New York: McGraw-Hill)
[34] Cubaud T and Mason T G 2006 *Phys. Rev. Lett.* **96** 114501
[35] Cubaud T and Mason T G 2008 *Phys. Rev.* E **78** 056308
[36] Cubaud T and Mason T G 2007 *Phys. Rev. Lett.* **98** 264501
[37] Johnson A M and Fletcher R C 1994 *Folding of Viscous Layers* (New York: Columbia University Press)
[38] Griffiths R W 2000 *Annu. Rev. Fluid Mech.* **32** 277
[39] Shah R K *et al* 2008 *Mater. Today* **11** 18
[40] Cubaud T and Mason T G 2007 *Phys. Fluids* **19** 091108
[41] Tritton D J 1988 *Physical Fluid Dynamics* (New York: Oxford University Press)